DALTON

# Ability of terephthalate (ta) to mediate exchange coupling in ta-bridged copper(II), nickel(II), cobalt(II) and manganese(II) dinuclear complexes

**Juan Cano,[a] Giovanni De Munno,*[,b] José Luis Sanz,[a] Rafael Ruiz,[a] Juan Faus,[a] Francesc Lloret,*[,†,a] Miguel Julve[a] and Andrea Caneschi[c]**

[a] *Departament de Química Inorgànica, Facultat de Química, Universitat de València, Dr. Moliner 50, 46100 Burjassot* (*València*), *Spain*
[b] *Dipartimento di Chimica, Università degli Studi della Calabria, 87030 Arcavacata di Rende* (*Cosenza*), *Italy*
[c] *Dipartimento di Chimica, Università degli Studi di Firenze, Via Maragliano 75/77, 50144 Firenze, Italy*

The exchange coupling between the unpaired electrons of divalent first-row transition-metal ions $M^{II}$ (M = Cu, Ni, Co or Mn) bridged by the terephthalate (ta) ligand (intramolecular metal–metal separation *ca.* 10 Å) has been systematically studied. The following complexes have been synthesized: $[Cu_2(bipy)_4(ta)][ClO_4]_2$ **1**, $[Cu_2(terpy)_2(H_2O)_2(ta)][ClO_4]_2$ **2**, $[Ni_2(bipy)_4(ta)][ClO_4]_2$ **3**, $[Co_2(bipy)_4(ta)][ClO_4]_2$ **4**, $[Mn_2(phen)_4(H_2O)_2(ta)][ClO_4]_2$ **5** and $[Mn_2(phen)_4(ta)][ClO_4]_2$ **6** (bipy = 2,2′-bipyridine, terpy = 2,2′:6′,2″-terpyridine, phen = 1,10-phenanthroline). Complexes **1**, **2**, **4** and **5** have been characterized by single-crystal X-ray analysis. Complex **6** was obtained by thermal dehydration of **5** at 60 °C or under vacuum at room temperature. The structures have in common the presence of cationic terephthalate-bridged $[M_2(ta)]^{2+}$ dinuclear units with bidentate (**1**, **3**–**6**) and terdentate (**2**) blocking ligands and unco-ordinated perchlorate counter ions. A co-ordinated water molecule per metal ion is present in complexes **2** and **5**. Variable-temperature magnetic susceptibility data for all the complexes have been measured over the range 2.0–298 K. In **1**–**5** only very weak antiferromagnetic coupling has been observed [*J ca.* −2.2 (**1**), −0.01 (**2**), −0.6 (**3**), −0.3 (**4**) and −0.065 $cm^{-1}$ (**5**), the Hamiltonian being $\hat{H} = -J\hat{S}_A \cdot \hat{S}_B$ with $S_A = S_B = \frac{1}{2}$ (**1**, **2**), 1 (**3**), $\frac{3}{2}$ (**4**) and $\frac{5}{2}$ (**5**)]. In contrast to the lack of magnetic interaction detected for complex **5**, a significant antiferromagnetic coupling ($J = -1.6$ $cm^{-1}$; maximum of susceptibility at 8.0 K) is observed in its dehydrated phase (**6**). The magnetostructural data and theoretical calculations demonstrate the low efficiency of terephthalate as a bridge to mediate exchange interactions between first-row transition-metal ions. The significant exchange coupling observed in **6** is due to the occurrence of a carboxylate bridge between the manganese(II) ions induced by a carboxylate-assisted loss of the co-ordinated water molecule.

The magnetostructural characterization of dinuclear copper(II) complexes has played a key role in the development of magnetochemistry.[1,2] One of the more appealing examples concerns the di-μ-hydroxo-dicopper(II) dimers where strong intramolecular ferro- or antiferro-magnetic interactions have been observed.[3,4] The possibility of achieving strong magnetic interactions between magnetic centres which are linked through more and more extended bridges actually appears as a very active area of molecular magnetism. In an attempt to investigate the dependence of *J* on the intramolecular metal–metal separation and thus to check if there is a limit distance for the exchange coupling to be propagated,[5] chemists have prepared a great variety of dinuclear copper(II) complexes where the intramolecular metal–metal separation is tuned in a wide range by using extended bridging ligands. Special attention has been paid to the bis-bidentate bridging groups of the oxalato type both from theoretical and experimental viewpoints. The oxalato bridge can mediate an antiferromagnetic coupling as large as −386 $cm^{-1}$ (singlet–triplet energy gap) between copper(II) ions separated by *ca.* 5 Å.[6–8] This antiferromagnetic coupling through oxalate can also be increased up to −800 $cm^{-1}$ by substituting the oxalato-oxygen atoms by less electronegative donor atoms such as nitrogen and sulfur, the intramolecular copper–copper separation being much larger (*ca.* 6 Å): the less electronegative the atoms of the bridge, the larger is the antiferromagnetic coupling.[9–12] For this family, the magnetic orbitals ($d_{x^2-y^2}$) are coplanar with the oxalato-type bridging unit. The oxocarbon dianions $C_nO_n^{2-}$ with $n = 4$ (squarate; 3,4-dihydroxycyclobut-3-ene-1,2-dionate)[13] and 5 (croconate; 4,5-dihydroxycyclopent-4-ene-1,2,3-trionate)[14] and hydranylate ($C_6O_4X_2^{2-}$; hydranilic acid when X = H)-type ligands[15] were used as bridging units in order to increase the copper–copper separation (6.8–7.8 Å), but they exhibit a much lower efficiency than oxalate. For all these cases simple orbital considerations[16] substantiated by extended-Hückel calculations provide a clear picture of the exchange pathway and thus an adequate explanation of the magnitude and nature of the observed coupling. Other more extended bridges with a greater number of atoms in the bridging skeleton such as 4,4′-bipyridine (intramolecular copper–copper separation about 11 Å)[17] were used but only weak antiferromagnetic interactions were observed. An interesting compound is $[Rh_2(O_2CCF_3)_4(tempo)_2]$ where two tempo organic radicals (tempo = 2,2,6,6-tetramethylpyridine 1-oxyl) interact through the singly bonded $Rh_2(O_2CCF_3)_4$ diamagnetic core.[18] The distance between the two nitroxyl oxygen atoms is 6.9 Å and the singlet–triplet energy gap is −478 $cm^{-1}$. In this case and in spite of the large distance between the magnetic centres, the antiferromagnetic interaction is propagated through only two rhodium atoms, (N–O)Rh–Rh(O–N). All these studies suggest that the antiferromagnetic coupling decreases as the number of atoms of the bridge increases rather than the distance.

A spectacular result was reported by Chaudhuri *et al.*[19]

† E-Mail: lloret@uv.es

dealing with the dinuclear copper(II) complex of formula $[Cu_2(tmtacn)_2(H_2O)_2(ta)][ClO_4]_2$ (tmtacn = 1,4,7-trimethyl-1,4,7-triazacyclononane, ta = dianion of terephthalic acid) where the metal atoms are bridged by the terephthalate ligand [eight atoms in the bridging skeleton (Cu–$OC_6O$–Cu), the intramolecular metal–metal distance being 11.3 Å]. The singlet–triplet splitting is reported to be $-140$ $cm^{-1}$, which is surprisingly too large especially in the light of the very weak antiferromagnetic coupling observed for other ta-bridged copper(II) dimers.[20–24]

The present work is devoted to the exchange pathway through the terephthalato bridge in a systematic fashion. To do that we have prepared the ta-bridged complexes of formula $[Cu_2(bipy)_4(ta)][ClO_4]_2$ **1**, $[Cu_2(terpy)_2(H_2O)_2(ta)][ClO_4]_2$ **2**, $[Ni_2(bipy)_4(ta)][ClO_4]_2$ **3**, $[Co_2(bipy)_4(ta)][ClO_4]_2$ **4**, $[Mn_2(phen)_4(H_2O)_2(ta)][ClO_4]_2$ **5** and $[Mn_2(phen)_4(ta)][ClO_4]_2$ **6** (bipy = 2,2′-bipyridine, terpy = 2,2′:6′,2″-terpyridine, phen = 1,10-phenanthroline) where the number and symmetry of the magnetic orbitals are varied. Their crystal structures and magnetic studies are presented herein. The crystal structure of complex **3** was reported previously.[25]

## Experimental

### Materials

The hexahydrate perchlorate salts of copper(II), nickel(II), cobalt(II) and manganese(II) and bipy and phen were from commercial sources and used as received. Piperidinium terephthalate[20] and the complex $[Ni_2(bipy)_4(ta)][ClO_4]_2$ **3**[25] were prepared by previously reported methods.

### Preparations

**$[Cu_2(bipy)_4(ta)][ClO_4]_2$ 1.** A solution of $[Cu(bipy)_2][ClO_4]_2$ (0.116 g, 0.2 mmol) and piperidinium terephthalate (0.034 g, 0.1 mmol) in methanol (200 $cm^3$) was heated at 60 °C with continuous stirring for 1 h and a sky-blue suspension was obtained. The small amount of the pale blue powder of formula $Cu(bipy)(ta)\cdot H_2O$ was filtered and the remaining solution was left to evaporate at room temperature in an open vessel. Prismatic blue crystals of **1** which were suitable for X-ray crystallography separated in a few days (Found: C, 51.45; H, 3.0; Cl, 6.15; Cu, 11.1; N, 9.9. Calc. for $C_{48}H_{36}Cl_2Cu_2N_8O_{12}$: C, 51.75; H, 3.25; Cl, 6.35; Cu, 11.4; N, 10.05%).

**$[Cu_2(terpy)_2(H_2O)_2(ta)][ClO_4]_2$ 2.** Piperidinium terephthalate (0.034 g, 0.1 mmol) dissolved in the minimum volume of methanol was slowly added to a warm methanolic solution (50 $cm^3$) of $Cu(ClO_4)_2\cdot 6H_2O$ (0.074 g, 0.2 mmol) and terpy (0.047 g, 0.2 mmol) with continuous stirring. After addition of hot water (20 $cm^3$), the resulting deep blue solution was left to evaporate in a hood at ambient temperature. Rhombohedral deep blue X-ray-quality crystals of complex **2** were grown in a few days (Found: C, 45.75; H, 2.9; Cl, 7.0; Cu, 12.55; N, 8.35. Calc. for $C_{38}H_{30}Cl_2Cu_2N_6O_{14}$: C, 46.0; H, 3.0; Cl, 7.15; Cu, 12.8; N, 8.45%).

**$[Co_2(bipy)_4(ta)][ClO_4]_2$ 4.** Piperidinium terephthalate (0.084 g, 0.25 mmol) dissolved in the minimum volume of methanol was slowly added to a warm methanolic solution (100 $cm^3$) of $Co(ClO_4)_2\cdot 6H_2O$ (0.183 g, 0.5 mmol) and bipy (0.156 g, 0.1 mmol) with continuous stirring. A clear deep orange solution was obtained from which an orange polycrystalline solid and reddish orange prismatic crystals of **3** separated in a few days on standing in an open vessel at room temperature (Found: C, 51.9; H, 3.0; Cl, 6.35; Co, 10.45; N, 9.9. Calc. for $C_{48}H_{36}Cl_2Co_2N_8O_{12}$: C, 52.15; H, 3.25; Cl, 6.4; Co, 10.65; N, 10.15%).

**$[Mn_2(phen)_4(H_2O)_2(ta)][ClO_4]_2$ 5 and $[Mn_2(phen)_4(ta)][ClO_4]_2$ 6.** The synthetic procedure to prepare complex **5** is analogous to that of **4** but using $Mn(ClO_4)_2\cdot 6H_2O$ and phen instead of $Co(ClO_4)_2\cdot 6H_2O$ and bipy. However, in the present case a highly insoluble yellow solid precipitated when adding the carboxylate. Analytical data were consistent with the formula $Mn(phen)(ta)\cdot H_2O$. From the resulting yellow solution, single crystals of **5** were grown as yellow needles in 2 d on standing at ambient temperature (Found: C, 54.35; H, 3.1; Cl, 5.5; Mn, 8.75; N, 9.0. Calc. for $C_{56}H_{40}Cl_2Mn_2N_8O_{14}$: C, 54.7; H, 3.25; Cl, 5.75; Mn, 8.95; N, 9.1%). The related compound **6** was obtained from **5** by thermal dehydration (loss of the two co-ordinated waters starts at 30 °C and is complete by 60 °C) or under vacuum over $P_2O_5$ at room temperature. Complex **6** is stable in the temperature range 60–280 °C and decomposes at higher temperatures.

### Physical techniques

The infrared spectra were taken on a Perkin-Elmer 1750 FTIR spectrophotometer as KBr pellets in the 4000–400 $cm^{-1}$ region. A Perkin-Elmer TAG-7 analyser was used to perform the dehydration of complex **5** in a nitrogen atmosphere and with a heating rate of 5° $min^{-1}$. Variable-temperature magnetic susceptibility data for polycrystalline samples of complexes **1**–**6** were obtained on a Metronique Ingenierie MS03 SQUID magnetometer over the temperature range 2.0–290 K and in a field of 1 T. The magnetometer was calibrated with $[NH_4]_2Mn[SO_4]_2\cdot 2H_2O$. The observed susceptibility data were corrected for the underlying diamagnetism by using Pascal's constants.

### Crystallography

Single crystals of complexes **1**, **2**, **4** and **5** with approximate dimensions 0.11 × 0.12 × 0.18 (**1**), 0.41 × 0.23 × 0.18 (**2**), 0.28 × 0.33 × 0.46 (**4**) and 0.35 × 0.18 × 0.12 mm (**5**) were used for data collection on a Siemens R3m/V automatic four-circle diffractometer with graphite-monochromated Mo-Kα radiation (λ = 0.710 73 Å) at 298 K. The cell parameters and crystal orientation matrices were obtained from least-squares refinement of 25 strong reflections in the range $15 \leqslant 2\theta \leqslant 30°$. Information concerning the crystallographic data collection and structure refinements is summarized in Table 1. Examination of two standard reflections, monitored every 150, showed no sign of crystal decay. Intensity data were corrected for Lorentz-polarization and absorption effects (ψ scans).[26] Reflections in the range 2θ 3–54 (**1**, **4** and **5**) and 3–55° (**2**) were measured in the ω–2θ scan mode.

The structures were solved by standard Patterson methods by means of the SHELXTL PLUS program[27] and subsequently completed by Fourier recycling. The function minimized during the full-matrix least-squares refinement was $\Sigma w(|F_o| - |F_c|)^2$. All non-hydrogen atoms [except the bipy carbon atoms from C(5) to C(24) for **1**] were refined anisotropically. The hydrogen atoms of the co-ordinated water molecule of complexes **2** and **5** were located in a $\Delta F$ map and refined with constraints. The other hydrogen atoms were set in calculated positions and refined as riding atoms. A common fixed isotropic thermal parameter was assigned to all hydrogen atoms. The final geometrical calculations were carried out with the PARST program.[28] The graphical manipulations were performed using the XP utility of the SHELXTL PLUS system. Main interatomic bond distances and angles for **1**, **2**, **4** and **5** are listed in Table 2.

Atomic coordinates, thermal parameters, and bond lengths and angles have been deposited at the Cambridge Crystallographic Data Centre (CCDC). See Instructions for Authors, *J. Chem. Soc.*, *Dalton Trans.*, 1997, Issue 1. Any request to the CCDC for this material should quote the full literature citation and the reference number 186/466.

## Results and Discussion

### Preparation of complexes

The yield of the synthesis of compounds **1**–**5** lies between 60

**Table 1** Crystallographic data and structure refinement for complexes **1**, **2**, **4** and **5**

| | **1** | **2** | **4** | **5** |
|---|---|---|---|---|
| Empirical formula | $C_{48}H_{36}Cl_2Cu_2N_8O_{12}$ | $C_{38}H_{30}Cl_2Cu_2N_6O_{14}$ | $C_{48}H_{36}Cl_2Co_2N_8O_{12}$ | $C_{56}H_{40}Cl_2Mn_2N_8O_{14}$ |
| $M$ | 1114.8 | 992.7 | 1105.6 | 1229.7 |
| Crystal system | Monoclinic | Triclinic | Monoclinic | Triclinic |
| Space group | $P2_1/c$ | $P\bar{1}$ | $P2_1/c$ | $P\bar{1}$ |
| $a$/Å | 12.472(5) | 7.313(2) | 13.086(2) | 8.337(2) |
| $b$/Å | 9.177(5) | 10.102(2) | 9.430(2) | 12.695(2) |
| $c$/Å | 21.565(6) | 14.599(2) | 20.246(3) | 13.566(2) |
| α/° | | 101.04(2) | | 97.15(2) |
| β/° | 108.31(3) | 103.05(2) | 108.84(1) | 104.32(2) |
| γ/° | | 103.35(2) | | 100.01(2) |
| $U$/Å$^3$ | 2322(2) | 987.9(4) | 2364.5(6) | 1229.7(4) |
| $Z$ | 2 | 1 | 2 | 1 |
| $D_c$/g cm$^{-3}$ | 1.595 | 1.668 | 1.553 | 1.514 |
| $F$(000) | 1136 | 504 | 1128 | 628 |
| μ(Mo-Kα)/mm$^{-1}$ | 1.106 | 1.290 | 0.888 | 0.643 |
| *hkl* Ranges | 0–15, −11 to 11, −27 to 25 | 0–9, −13 to 12, −18 to 18 | 0–16, −12 to 0, −25 to 24 | 0–10, −16 to 16, −17 to 16 |
| Maximum, minimum transmission | 0.822, 0.728 | 0.821, 0.698 | 0.802, 0.721 | 0.882, 0.866 |
| No. reflections collected | 10 374 | 4991 | 6003 | 6436 |
| No. unique reflections | 5102 | 4564 | 5194 | 5925 |
| $R_{int}$ | 0.010 | 0.032 | 0.018 | 0.015 |
| No. observed reflections [$I > 3\sigma(I)$] | 2003 | 3667 | 3149 | 3078 |
| Weighting scheme, $w^{-1}$ | $\sigma^2(F_o) + 0.0010F_o^2$ | $\sigma^2(F_o) + 0.0008F_o^2$ | $\sigma^2(F_o) + 0.0027F_o^2$ | $\sigma^2(F_o) + 0.0006F_o^2$ |
| No. parameters refined | 225 | 286 | 325 | 376 |
| Largest and mean Δ/σ | 0.001, 0.000 | 0.002, 0.001 | 0.003, 0.001 | 0.012, 0.002 |
| Largest difference peak, hole/e Å$^{-3}$ | 0.41, −0.56 | 0.76, −0.47 | 0.59, −0.42 | 0.70, −0.32 |
| $R$ | 0.056 | 0.036 | 0.042 | 0.052 |
| $R'$ | 0.058 | 0.041 | 0.049 | 0.055 |
| Goodness of fit | 1.20 | 1.39 | 0.97 | 1.59 |

$R = \Sigma(||F_o| - |F_c||)/\Sigma|F_o|$; $R' = [\Sigma w(|F_o| - |F_c|)^2/\Sigma wF_o^2]^{\frac{1}{2}}$; goodness of fit = $[\Sigma w(|F_o| - |F_c|)^2/(N_o - N_p)]^{\frac{1}{2}}$, $N_o$ = number of observations, $N_p$ = number of parameters.

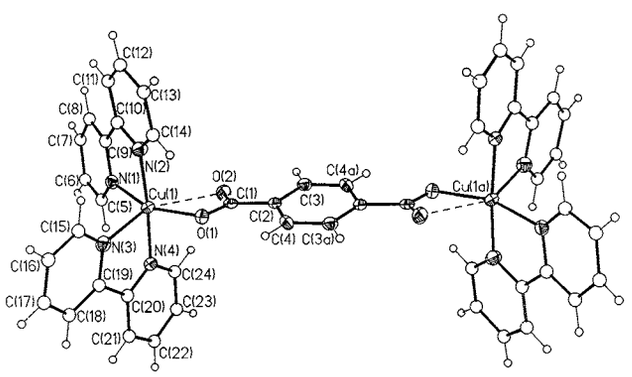


**Fig. 1** Perspective view of the cationic unit $[Cu_2(bipy)_4(ta)]^{2+}$ of complex **1** showing the atom labelling. Thermal ellipsoids are drawn at the 30% probability level. The broken lines indicate the weak interaction between the $Cu^{II}$ and O(2) carbonyl oxygen of the co-ordinated carboxylate

and 70%. Single crystals of them were selected and used for the magnetic measurements in order to avoid contaminants. In fact, although the terephthalate was slowly added to the warm metal-containing solutions with continuous stirring, the formation of insoluble polymers of composition $(ML)_2(ta)\cdot nH_2O$ occurs in the case of complexes **1** and **5**. Our synthetic results are in accord with the difficulties found by other authors in obtaining parent copper(II) dinuclear complexes.[24]

According to their crystal structures, compounds **1**–**5** have in common the occurrence of the ta-bridged $[M_2(ta)]^{2+}$ dinuclear unit and unco-ordinated perchlorate anions. The terephthalate group acts as a bis-bidentate ligand in **1**, **3** and **4**. The values of the difference between the ν(C=O) and ν(C–O) stretching frequencies (Δ) in the infrared spectra of these compounds [160 (**1**), 135 (**3**) and 140 cm$^{-1}$ (**4**)] are all significantly lower than those reported for the free carboxylate, as expected for the case of a chelating carboxylate.[29] The terephthalate ligand in complexes **2** and **5** adopts a bis-monodentate co-ordination mode. This structural feature accounts for the values of Δ observed in their IR spectra, 200 cm$^{-1}$ for **2** and 185 cm$^{-1}$ for **5**. The occurrence of a hydrogen bond between the free carboxylate oxygen and a co-ordinated water molecule allows the carboxylato conformation to be *syn-anti* (**2**) and *syn-syn* (**5**). Finally, as far as the IR spectrum of the anhydrous compound $[Mn_2(phen)_4(ta)][ClO_4]_2$ **6** (obtained by gentle heating of a small amount of **5** at 60° C or under vacuum), apart from the lack of the water peaks, the most important feature is that the value of Δ is practically the same as that of **5**. This fact excludes the possibility of bis-bidentate terephthalate in **6** and strongly supports the occurrence of the tetrakis-monodentate co-ordination mode as in the related $[Mn_2(bipy)_4(ta)][ClO_4]_2$ **7** (Δ = 185 cm$^{-1}$),[30] which was reported by us recently and shows the occurrence of two carboxylato-bridges in the *syn-syn* conformation between a pair of manganese(II) ions.

## Crystal structures

The structures of compounds **1**, **2**, **4** and **5** are made up of ta-bridged dinuclear cations with bipy (**1** and **4**), terpy (**2**) and phen (**5**) as terminal ligands, and non-co-ordinated perchlorate counter ions. One co-ordinated water molecule per metal ion is present in the structures of **2** and **5**. Perspective drawings of the dinuclear entities of these compounds are shown in Figs. 1 (**1**), 2(*a*) (**2**), 3 (**4**) and 4 (**5**). All dimers lie about a crystallographic centre which is located at the middle of the benzene ring of the ta ligand. It should be noted that **1**, **3** and **4** are isostructural. The dinuclear entities in **2** are linked by a hydrogen bond involving the unco-ordinated carboxylate of one unit and the co-ordinated water molecule of another [2.746(3) Å and 177(3)° for O(1b)···O(3) and O(1b)···H(1w)–O(3), respectively;

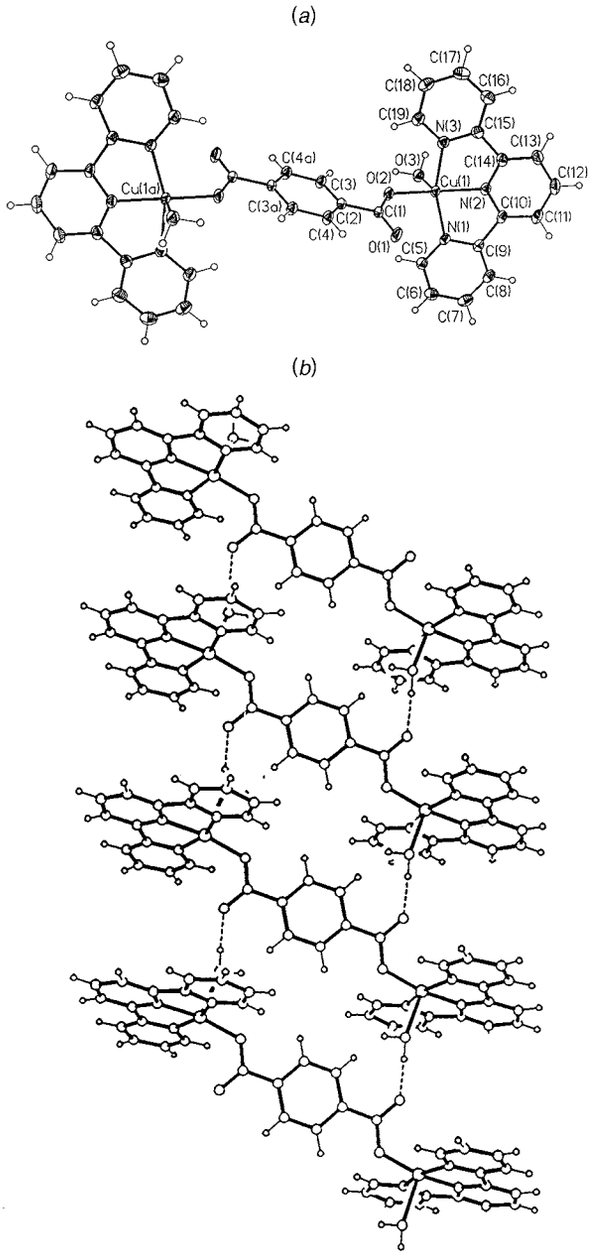


**Fig. 2** (*a*) Perspective view of the cationic unit $[Cu_2(terpy)_2(H_2O)_2(ta)]^{2+}$ of complex **2** showing the atom labelling. Thermal ellipsoids are drawn at the 30% probability level. (*b*) A view of the intermolecular hydrogen bonding linking the dinuclear $[Cu_2(terpy)_2(H_2O)_2(ta)]^{2+}$ units

symmetry relation b $1 + x, y, z$] leading to a double chain along the *x* axis [see Fig. 2(*b*)]. A strong hydrogen bond occurs between the co-ordinated water and the unco-ordinated carboxylate oxygens in **5** [2.617(1) Å and 151(3)° for O(3)···O(2) and O(3)–H(2w)···O(2), respectively] yielding a six-membered ring. The terephthalate adopts bis-bidentate (**1**, **4**) or bis-monodentate (**2**, **5**) co-ordination modes.

The metal environment of complexes **1** and **4** can be described as a distorted octahedron with one carboxylato-oxygen [O(1)] of the ta ligand and three bipy-nitrogen atoms [N(1), N(2) and N(4)] that comprise the equatorial plane, whereas the axial positions are filled by the remaining bipy nitrogen [N(3)] and the other carboxylato-oxygen atoms [O(2)]. The largest deviations from the mean N(1)N(2)O(1)N(4) equatorial plane are 0.268(7) [(N2) for **1**] and 0.224(7) Å [N(1) for **2**]. The metal atom is displaced toward the apical site by 0.193(1) (**1**) and 0.131(1) Å (**4**) [0.133(1) Å in **3**]. In both compounds the main distortion from the octahedral geometry is due to the small bite angle of the carboxylate group [54.5(2) (**1**) and 60.5(1)° (**4**); 61.9(1)° in **3**]. The Jahn–Teller effect which is present in the copper(II) complexes accounts for the pronounced axial elongation in **1** with respect to **4** [2.650(6) Å for Cu(1)–O(2) in **1** against 2.176(3) Å for Co(1)–O(2) in **4** and 2.144(3) Å for Ni(1)–O(2) in **3**]. This is also related to the different values of the N(1)–Cu(1)–O(1) and N(1)–Co(1)–O(1) bond angles [155.7(2) and 160.2(1)°, respectively; the corresponding value in **3** is 161.5(1)°]. The Jahn–Teller effect in **1** also accounts for the lengthening of the Cu(1)–N(3) bond with respect to Cu(1)–N(1), Cu(1)–N(2) and Cu(1)–N(4). The values of the metal to carboxylate oxygen distances in **4** (average 2.16 Å)

**Table 2** Selected bond lengths (Å) and interbond angles (°) for complexes **1**, **2**, **4** and **5**

| | | | |
|---|---|---|---|
| Complex **1** | | | |
| Cu(1)–O(1) | 1.997(6) | Cu(1)–N(3) | 2.169(7) |
| Cu(1)–O(2) | 2.650(6) | Cu(1)–N(4) | 2.004(5) |
| Cu(1)–N(1) | 2.058(7) | O(1)–C(1) | 1.285(10) |
| Cu(1)–N(2) | 1.985(6) | O(2)–C(1) | 1.229(11) |
| O(1)–Cu(1)–N(1) | 155.7(2) | N(1)–Cu(1)–N(2) | 80.3(3) |
| O(1)–Cu(1)–N(2) | 92.0(3) | N(1)–Cu(1)–N(3) | 104.7(3) |
| O(1)–Cu(1)–N(3) | 99.2(3) | N(1)–Cu(1)–N(4) | 96.0(3) |
| O(1)–Cu(1)–N(4) | 92.7(2) | N(2)–Cu(1)–N(3) | 99.6(3) |
| O(1)–Cu(1)–O(2) | 54.5(2) | N(2)–Cu(1)–N(4) | 175.1(3) |
| O(2)–Cu(1)–N(1) | 102.9(2) | N(3)–Cu(1)–N(4) | 78.2(2) |
| O(2)–Cu(1)–N(2) | 94.7(2) | Cu(1)–O(1)–C(1) | 105.9(5) |
| O(2)–Cu(1)–N(3) | 150.6(2) | Cu(1)–O(2)–C(1) | 76.8(5) |
| O(2)–Cu(1)–N(4) | 89.2(2) | O(1)–C(1)–O(2) | 122.5(8) |
| Complex **2** | | | |
| Cu(1)–O(2) | 1.900(2) | Cu(1)–N(3) | 2.023(3) |
| Cu(1)–O(3) | 2.290(2) | O(1)–C(1) | 1.235(3) |
| Cu(1)–N(1) | 2.010(2) | O(2)–C(1) | 1.270(3) |
| Cu(1)–N(2) | 1.932(2) | | |
| O(2)–Cu(1)–O(3) | 90.2(1) | O(3)–Cu(1)–N(3) | 97.0(1) |
| O(2)–Cu(1)–N(1) | 103.8(1) | N(1)–Cu(1)–N(2) | 80.6(1) |
| O(2)–Cu(1)–N(2) | 165.8(1) | N(1)–Cu(1)–N(3) | 160.4(1) |
| O(2)–Cu(1)–N(3) | 94.5(1) | N(2)–Cu(1)–N(3) | 80.0(1) |
| O(3)–Cu(1)–N(1) | 89.9(1) | Cu(1)–O(2)–C(1) | 121.8(2) |
| O(3)–Cu(1)–N(2) | 103.5(1) | O(1)–C(1)–O(2) | 124.8(2) |
| Complex **4** | | | |
| Co(1)–O(1) | 2.148(3) | Co(1)–N(3) | 2.107(3) |
| Co(1)–O(2) | 2.176(3) | Co(1)–N(4) | 2.108(3) |
| Co(1)–N(1) | 2.103(3) | O(1)–C(1) | 1.260(5) |
| Co(1)–N(2) | 2.106(3) | O(2)–C(1) | 1.260(5) |
| O(1)–Co(1)–O(2) | 60.5(1) | N(1)–Co(1)–N(2) | 77.9(1) |
| O(1)–Co(1)–N(1) | 160.2(1) | N(1)–Co(1)–N(3) | 101.7(1) |
| O(1)–Co(1)–N(2) | 92.8(1) | N(1)–Co(1)–N(4) | 98.7(1) |
| O(1)–Co(1)–N(3) | 96.9(1) | N(2)–Co(1)–N(3) | 98.7(1) |
| O(1)–Co(1)–N(4) | 91.8(1) | N(2)–Co(1)–N(4) | 174.2(1) |
| O(2)–Co(1)–N(1) | 102.3(1) | N(3)–Co(1)–N(4) | 77.3(1) |
| O(2)–Co(1)–N(2) | 93.9(1) | Co(1)–O(1)–C(1) | 90.6(2) |
| O(2)–Co(1)–N(3) | 154.7(1) | Co(1)–O(2)–C(1) | 89.3(2) |
| O(2)–Co(1)–N(4) | 91.4(1) | O(1)–C(1)–O(2) | 119.6(4) |
| Complex **5** | | | |
| Mn(1)–O(1) | 2.120(3) | Mn(1)–N(3) | 2.291(4) |
| Mn(1)–O(3) | 2.141(4) | Mn(1)–N(4) | 2.256(4) |
| Mn(1)–N(1) | 2.272(4) | O(1)–C(1) | 1.265(6) |
| Mn(1)–N(2) | 2.281(4) | O(2)–C(1) | 1.243(6) |
| O(1)–Mn(1)–O(3) | 86.3(1) | N(1)–Mn(1)–N(2) | 73.0(1) |
| O(1)–Mn(1)–N(1) | 87.7(1) | N(1)–Mn(1)–N(3) | 93.2(2) |
| O(1)–Mn(1)–N(2) | 106.5(1) | N(1)–Mn(1)–N(4) | 98.7(1) |
| O(1)–Mn(1)–N(3) | 88.1(1) | N(2)–Mn(1)–N(3) | 159.1(2) |
| O(1)–Mn(1)–N(4) | 160.3(1) | N(2)–Mn(1)–N(4) | 93.2(1) |
| O(3)–Mn(1)–N(1) | 163.6(2) | N(3)–Mn(1)–N(4) | 73.0(2) |
| O(3)–Mn(1)–N(2) | 94.1(1) | Mn(1)–O(1)–C(1) | 131.7(3) |
| O(3)–Mn(1)–N(3) | 101.9(1) | O(1)–C(1)–O(2) | 125.6(5) |
| O(3)–Mn(1)–N(4) | 92.0(1) | | |

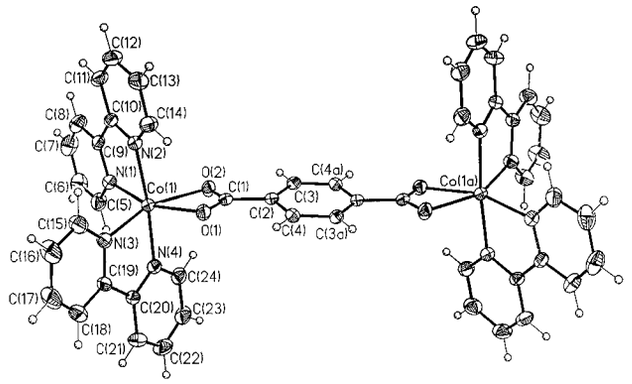


**Fig. 3** Perspective view of the cationic unit $[Co_2(bipy)_4(ta)]^{2+}$ of complex **4** showing the atom labelling. Thermal ellipsoids are drawn at the 30% probability level

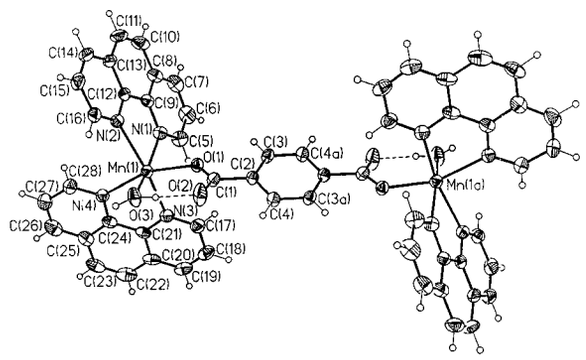


**Fig. 4** Perspective view of the cationic unit $[Mn_2(phen)_4(H_2O)_2(ta)]^{2+}$ of complex **5** showing the atom labelling. Thermal ellipsoids are drawn at the 30% probability level. The broken lines indicate the intramolecular hydrogen bond between the co-ordinated water molecule and the carbonyl oxygen atom of the co-ordinated carboxylate

are similar to the related ones in **3** (mean 2.13 Å) but both are significantly larger than the shortest copper to carboxylate oxygen bond in **1** [1.997(6) Å]. The values of the angle subtended at the metal atom by the chelating bipy exhibit large deviations from the orthogonal geometry [80.3(3) and 78.2(2)° (**1**) and 77.9(1) and 77.3(1)° (**4**); 79.8(2) and 79.4(2)° in **3**] as expected due to the small bite angle of the bipy ligand.[31]

The copper atom in complex **2** exhibits a distorted square-pyramidal geometry. The three terpy nitrogen [N(1), N(2) and N(3)] and one carboxylate oxygen [O(2)] atoms comprise the basal plane. The apex of the pyramid is occupied by the oxygen atom [O(3)] of the water molecule. The axial metal–oxygen distance [2.290(2) Å for Cu(1)–O(3)] is somewhat longer than the equatorial one [1.900(2) Å for Cu(1)–O(2)]. The copper–oxygen (carboxylate) bond distance is the shortest for reported bis-monodentate ta-bridged copper(II) complexes.[19,20,22,24,32] The pattern exhibited by the values of the copper to terpy-nitrogen bond lengths (two approximately equal bond distances for the metal to outer pyridine nitrogens and a significantly shorter metal to middle pyridine nitrogen) is in agreement with that reported for other terpy-containing copper(II) complexes.[33,34] The largest deviation from the mean N(1)N(2)N(3)O(2) basal plane is 0.084(3) Å for N(3). The metal atom is displaced toward the apical site by 0.160(1) Å. The values of the angles at the metal atom in the two five-membered chelate rings deviate significantly from 90° [80.0(1) and 80.6(1)° for N(2)–Cu(1)–N(3) and N(1)–Cu(1)–N(2)] because the geometrical constraints of the tridentate terpy ligand.

Each manganese atom in complex **5** presents a distorted octahedral geometry. Three phen nitrogen atoms [N(2), N(3) and N(4)] and a carboxylate-oxygen atom [O(1)] comprise the best equatorial plane of the octahedron, whereas the axial positions are filled by the remaining phen nitrogen atom [N(1)] and the oxygen atom [O(3)] of the co-ordinated water molecule. The Mn–O (carboxylate) bond distance [2.120(3) Å] is somewhat shorter than Mn–N (phen) [2.291(4)–2.256(4) Å] but very similar to that observed in the parent compound **7** [average 2.118(2) Å for Mn–O (carboxylate)].[30] The main distortion from the octahedral symmetry is due to the reduced bite angle of the phen ligand [73.0(2)° for N(1)–Mn(1)–N(2) and N(3)–Mn(1)–N(4)], which is in agreement with those found in other phen-containing manganese(II) complexes.[35,36] The largest deviation from the best N(2)O(1)N(3)N(4) equatorial plane is 0.233(4) Å for the N(3) atom; Mn(1) is displaced out of this plane by 0.106(1) Å.

The ta ligand in complexes **1**–**5** is quasi-planar [dihedral angle between the carboxylate group and the benzene ring 10.2(3) (**1**), 9.6(1) (**2**), 5.2(3) (**3**), 5.7(1) (**4**) and 13.6(2)° (**5**)]. The carboxylate group shows the expected trigonal geometry. However, significant differences are observed in the values of the carbon–oxygen bond distance and O(1)–C(1)–O(2) intra-carboxylate bond angle: these values are 1.260(5) Å and 120° for the symmetrical chelating carboxylato co-ordination (**3** and **4**), whereas two different carbon–carboxylate bonds and a larger intracarboxylate bond angle occur for the asymmetrical chelating [1.28(1) and 1.23(1) Å and 122.5(8)° (**1**)] and monodentate carboxylate co-ordination [1.235(3) and 1.270(3) Å and 124.8(2)° (**2**); 1.265(6) and 1.243(6) Å and 125.6(5)° (**5**)].

The pyridyl rings of bipy and terpy are planar as the phen ligand [deviations not greater than 0.010(3) Å for terpy, 0.025(11) Å for bipy in **1**, 0.020(5) Å for bipy in **4** and 0.024(7) Å for phen]. The bipy and terpy ligands as a whole are quite planar, the dihedral angles between the pyridyl rings being 10.1(2) and 3.9(3)° in **1**, 5.1(1) and 1.0(1)° in **4**, and 1.1(1), 1.4(1) and 1.3(1)° in **2**. Bond distances and angles within the bipy, terpy and phen ligands are as expected and in agreement with previously reported values.[31,33–36]

The intradimer metal–metal separation is 11.004(4) (**1**), 10.913(3) (**2**), 10.763(2) (**4**) and 11.457(3) Å (**5**) [9.449 Å (**3**)]. The shortest metal–metal separations through different units are 7.688(3) Å for Cu(1)···Cu(1b) (symmetry code: b $-x$, $-y$, $-z$) in **1**, 7.272(1) Å for Cu(1)···Cu(1b) (symmetry code: b $1-x$, $1-y$, $1-z$) in **2**, 7.398(1) Å for Co(1)···Co(1b) (symmetry code: b $-x$, $-y$, $-z$) in **4**, 8.337(2) Å for Mn(1)···Mn(1b) and Mn(1)···Mn(1c) (symmetry codes: b $x-1$, $y$, $z$; c $x+1$, $y$, $z$) in **5**.

The perchlorate anions have their expected tetrahedral geometry [average Cl–O and O–Cl–O 1.408(4) Å and 109.5(2)° for **1**, 1.425(10) Å and 109.4(6)° for **2**, 1.416(6) Å and 109.4(4)° for **4**, 1.403(6) Å and 109.5(3)° for **5**]. Hydrogen bonds involving the co-ordinated water molecule of **2** and **5** and the perchlorate O(4) [3.066(4) Å and 161(2)° for O(4)···O(3) and O(4)···H(2w)–O(3), respectively] and O(7) [2.776(7) Å and 149(3)° for O(7)···O(3) and O(7)···H(1w)–O(3), respectively] oxygen atoms are present.

## Magnetic properties

The temperature dependence of the $\chi_m T$ product ($\chi_m$ being the molar magnetic susceptibility) for the dinuclear complexes **1**–**3** is shown in Fig. 5. At 290 K, $\chi_m T = 0.87$ (**1**), 0.89 (**2**) and 2.21 (**3**) cm$^3$ K mol$^{-1}$, consistent with two uncoupled copper(II) (**1**, **2**) and nickel(II) (**3**) ions. Upon cooling, $\chi_m T$ for **2** remains nearly constant thus exhibiting a quasi-Curie law. However, $\chi_m T$ for the other two complexes decreases significantly at $T < 20$ (**1**) and < 40 K (**2**) and reaches values of 0.51 cm$^3$ K mol$^{-1}$ at 2.4 K for **1** and 1.90 cm$^3$ K mol$^{-1}$ at 2.7 K for **3**. The magnetic parameters $J$ (singlet–triplet energy gap) and $g$ for complexes **1** and **2** were estimated from a least-squares fitting of the susceptibility data by the corresponding Bleaney–Bowers expression derived through the Hamiltonian $\hat{H} = -J\hat{S}_A \cdot \hat{S}_B$ with $S_A = S_B = \frac{1}{2}$. The results of the fit are summarized in Table 3 together with some pertinent structural data. The magnetic data for complex **3**

**Table 3** Selected magnetostructural data for complexes **1**–**6**

| Complex | $J$/cm$^{-1}$ | $g$ | ρ[a] | $10^5R$[b] | $-n^2J$ | α[c]/° | β[c]/° | γ[c]/° | $d_{intra}$[d]/Å | $d_{inter}$[e]/Å |
|---|---|---|---|---|---|---|---|---|---|---|
| **1** | −2.2 | 2.07 | 0.3 | 4.1 | 2.20 | 10.2 | 10.0 | | 11.0 | 7.7 |
| **2** | −0.01 | 2.09 | 0 | 2.2 | 0.01 | 9.6 | 23.1 | | 10.9 | 7.3 |
| **3** | −0.6 ($D$ = 2) | 2.11 | 0.2 | 6.4 | 2.40 | 5.2 | 1.4 | 7.9 | 9.5 | 7.3 |
| **4**[f] | −0.33 | $g_{\parallel}$ = 8.12<br>$g_{\perp}$ = 1.29 | 0 | 11 | 2.97 | 5.7 | 2.3 | 9.6 | 10.8 | 7.4 |
| **5** | −0.065 | 1.99 | 0 | 1.8 | 1.63 | 13.6 | 25.2 | 24.8 | 11.5 | 8.3 |
| **6** | −1.6 | 1.99 | 0.8 | 3.2 | 40.0 | | | | | |

[a] Percentage of mononuclear copper(II) impurity. [b] Agreement factor defined as $\Sigma_i[\chi_m^{exptl}(i) - \chi_m^{calc}(i)]^2/\Sigma_i[\chi_m^{exptl}(i)]^2$. [c] α, β and γ are the dihedral angles shown in Scheme 1. [d] Intramolecular metal–metal separation. [e] Shortest intermolecular metal–metal separation. [f] Fitting through the Ising model (see text).

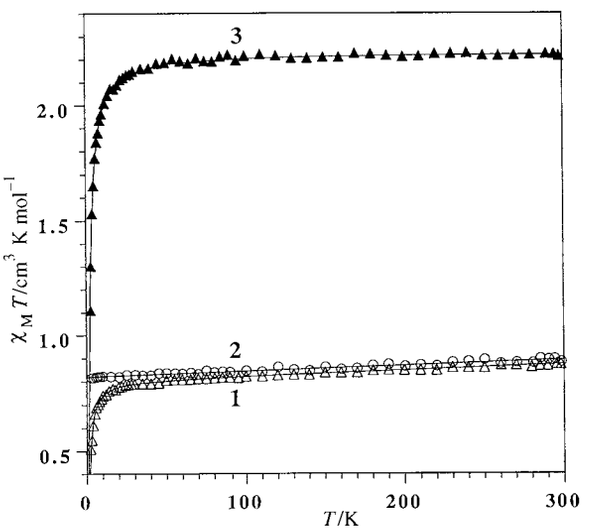


**Fig. 5** Temperature dependence of $\chi_m T$ of solid samples of complexes **1**–**3**. The solid line represents the best fit (see text)

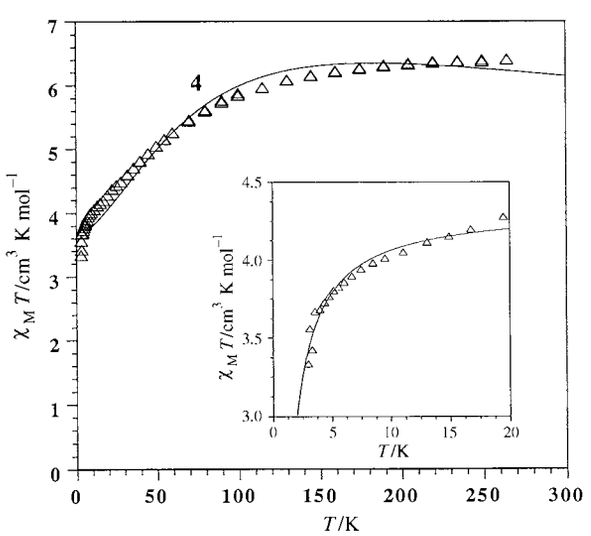


**Fig. 6** Temperature dependence of $\chi_m T$ of solid sample of complex **4**. The solid line corresponds to the best fit through the Lines model (see text). The inset shows the low-temperature region and the solid line represents the best fit to the magnetic data for an Ising dimer ($S_{eff} = \frac{1}{2}$)

were treated by the theoretical expression derived through the Hamiltonian $\hat{H} = -J\hat{S}_A \cdot \hat{S}_B - D\ (\hat{S}_{zA}^2 + \hat{S}_{zB}^2)$[37,38] where $S_A = S_B = 1$, $D$ is the single-ion zero-field splitting and it was assumed that $g_x = g_y = g_z = g$. The values of the variable parameters $J$, $D$ and $g$ resulting from the least-squares fitting are listed in Table 3.

The thermal dependence of the $\chi_m T$ for complex **4** is shown in Fig. 6. The value of $\chi_m T$ is 6.40 cm$^3$ K mol$^{-1}$ at 290 K and it decreases continuously when cooling, reaching a value of 3.30

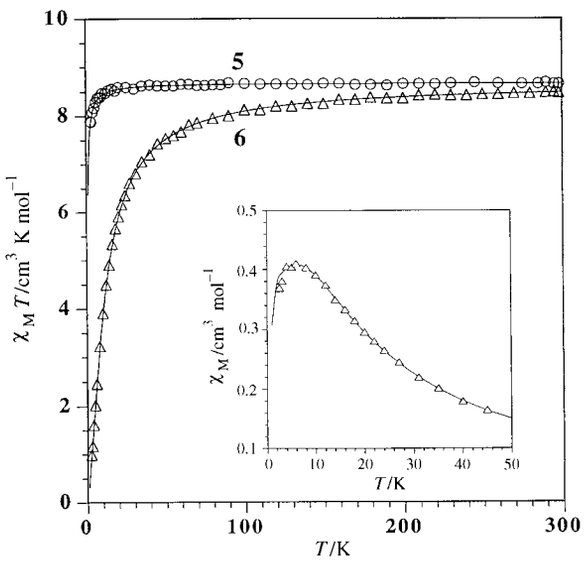


**Fig. 7** Temperature dependence of $\chi_m T$ of solid samples of complexes **5** and **6** (the solid line corresponds to the best fit). The inset shows the temperature variation of the susceptibility of **6** in the low-temperature region

cm$^3$ K mol$^{-1}$ at 2.9 K. This is indicative that an antiferromagnetic coupling occurs. The susceptibility curve does not exhibit any maximum. The value of $\chi_m T$ at room temperature is larger than that expected for the spin-only formula indicating that an important orbital contribution is involved. In fact, all our attempts to reproduce the susceptibility data through an isotropic Heisenberg form of interaction were unsuccessful. Therefore, the Lines theory[39] was used to treat the whole variable-temperature magnetic data. In so doing the experimental curve was only roughly reproduced with the magnetic parameters $J = -0.36$ cm$^{-1}$, $x$ (orbital reduction factor) = 0.88 and λ (spin–orbit coupling) = −99 cm$^{-1}$. The slight disagreement between the experimental and computed curves can be attributed to the fact that the Lines theory does not take into account any distortion of high-spin cobalt(II) from the octahedral geometry. Since it is possible to assume that for $T$ < 30 K only the Kramer's doublet for cobalt(II) is populated, this system can be treated as an Ising dimer.[40,41] The results of the fit are listed in Table 3 and the good quality of the fit is illustrated by the inset of Fig. 6. It should be noted that both the Lines and Ising approaches lead to practically identical $J$ values.

The magnetic behaviour of complexes **5** and **6** in the form of a plot of $\chi_m T$ *versus* $T$ is shown in Fig. 7. At 290 K, $\chi_m T$ for **5** is 8.70 cm$^3$ K mol$^{-1}$, very similar to that expected for two non-interacting manganese(II) ions (8.75 cm$^3$ K mol$^{-1}$). In the case of **6**, $\chi_m T$ at room temperature is 8.50 cm$^3$ K mol$^{-1}$. For both complexes $\chi_m T$ continuously decreases upon cooling and reaches a value of 7.90 cm$^3$ K mol$^{-1}$ at 2.7 K for **5** and of 1.0 cm$^3$ K mol$^{-1}$ at 2.5 K for **6**. This behaviour is characteristic of an antiferromagnetic interaction between two high-spin man-

**Table 4** Structural and magnetic data of terephthalato-bridged copper(II) complexes

| Compound[a] | $J$[b]/cm$^{-1}$ | α/° | β/° | $d_{intra}$/Å | $d_{inter}$/Å | Ref. |
|---|---|---|---|---|---|---|
| $[Cu_2(bipy)_4(\mu\text{-ta})][ClO_4]_2\cdot 2H_2O$[d] | +2.22 | | | | | 42 |
| $[Cu_2(L^1)_2(\mu\text{-ta})]\cdot H_2O\cdot MeOH$ | +0.6 | 5.8 | 7.7 | 11.0 | 8.8 | 22 |
| $[Cu_2(pedien)_2(H_2O)_2(\mu\text{-ta})][ClO_4]_2\cdot H_2O$ | 0 | 25 | 1.5 | 10.7 | 8.1 | 20 |
| $[Cu(mpy)_2(\mu\text{-ta})]\cdot 0.5(mpy)\cdot 0.5MeOH$ | 0 | 3.6 | 3.5 | 10.6 | 4.4 | 43 |
| $[Cu_2(terpy)_2(H_2O)_2(\mu\text{-ta})][ClO_4]_2$ | −0.01 | 9.6 | 23.1 | 10.9 | 7.3 | This work |
| $[Cu(en)(H_2O)_2(\mu\text{-ta})]$ | *c* | 10.6 | 3.0 | 11.2 | 5.7 | 32 |
| $[Cu_2(bipy)_4(\mu\text{-ta})][PF_6]_2\cdot 2H_2O$[d] | −0.88 | | | | | 42 |
| $[Cu_2(phen)_4(\mu\text{-ta})][ClO_4]_2\cdot 2H_2O$[d] | −1 | | | | | 42 |
| $[Cu_2(bipy)_4(\mu\text{-ta})][ClO_4]_2$ | −2.2 | 10.2 | 10.0 | 11.0 | 7.7 | This work |
| $[Cu_2(pmdien)_2(H_2O)_2(\mu\text{-ta})][ClO_4]_2$ | −2.7 | 10.4 | 6.9 | 11.1 | 7.8 | 20 |
| $[Cu_2(tmtacn)_2(SCN)_2(\mu\text{-ta})][ClO_4]_2\cdot 2MeOH$ | −2.8 | 18.4 | | 11.2 | 8.0 | 24 |
| $[Cu_2(dien)_2(\mu\text{-ta})][ClO_4]_2$ | −3.41 | 38.1 | 0.5 | 11.0 | 4.2 | 21 |
| $[Cu_2(trien)_2(\mu\text{-ta})][ClO_4]_2$[d] | −4.4 | | | | | 42 |
| $[Cu_2(bipy)_2(H_2O)_2(\mu\text{-ta})][ClO_4]_2$[d] | −51.8 | | | | | 23 |
| $[Cu_2(tmtacn)_2(H_2O)_2(\mu\text{-ta})][ClO_4]_2$ | −140 | 8.8 | 6.1 | 11.3 | 7.6 | 24 |

[a] Ligand abbreviations: $L^1$ = *N*-[2-(diethylamino)ethyl]salicylidenaminate; pedien = *N*,*N*,*N*′,*N*″,*N*″-pentaethyldiethylenetriamine; mpy = 3-methylpyridine; en = ethane-1,2-diamine; pmdien = *N*,*N*,*N*′,*N*″,*N*″-pentamethyldiethylenetriamine; tmtacn = 1,4,7-trimethyl-1,4,7-triazacyclononane; dien = diethylenetriamine; trien = triethylenetetramine. [b] The coupling constant, *J*, as defined by the Hamiltonian $\hat{H} = -J\hat{S}_1\hat{S}_2$; $S_1 = S_2 = \frac{1}{2}$. [c] Weakly antiferromagnetic. [d] Structure unknown.

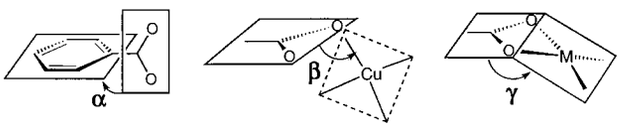


**Scheme 1**

ganese(II) ions, that occurring in **6** being stronger than that in **5**. The presence of a sharp susceptibility maximum around 6 K (see inset of Fig. 7) for **6** is the signature of an antiferromagnetic interaction with a singlet ground state. The susceptibility data for both complexes were treated by the isotropic Heisenberg $S_A = S_B = \frac{5}{2}$ spin-coupled dimer model ($\hat{H} = -J\hat{S}_A\cdot\hat{S}_B$) and the computed curves match very well the experimental data as shown in Fig. 7. The values of the magnetic parameters *J* and *g* are listed in Table 3.

All the ta-bridged copper(II) complexes known are listed in Table 4 together with selected magnetostructural data. It can be seen that the magnetic interaction is very weak ($|J| \leqslant 4$ cm$^{-1}$) except for the two last examples. The weak coupling observed is not surprising in the light of the large intramolecular metal–metal separation (>10.6 Å). This feature is not limited to copper(II) as shown in the present work where for the first time magnetic ions other than copper(II) (complexes **3**–**6** in Table 3) possessing a greater number of magnetic orbitals have been investigated. In the light of the data gathered in Tables 3 and 4 three main questions arise: (i) is there any influence of the structural parameters on the magnitude of the coupling?; (ii) what is the reason for the decrease in the magnetic interaction when the number of magnetic orbitals increases as shown in Table 3 when going from copper(II) to manganese(II)?; (iii) most interestingly, why do complex **6** in Table 3 as well as the two last compounds in Table 4 present relatively large antiferromagnetic interactions?

In order to answer the first question, the intra- and intermolecular metal–metal separations and the values of the dihedral angles α, β and γ, defined in Scheme 1, were included in Tables 3 and 4. It is clear that the greater the intramolecular metal–metal separation and the α, β and γ dihedral angles, the weaker the magnetic coupling should be. Complexes in Table 4 have been ordered according to the increasing antiferromagnetic coupling. Given that the intramolecular metal–metal separation is practically constant in this series and that the values of the dihedral angles do not follow the expected trend, both factors should not play a significant role. Owing to the very weak antiferromagnetic coupling observed in them and, consequently, the most likely large errors associated with the

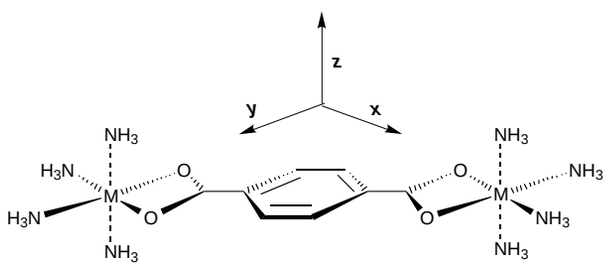


**Scheme 2**

quoted *J* values, our feeling is that additional comments are out of order. In spite of the large variation of the intermolecular metal–metal separation (from 8.8 to 4.2 Å), the values of *J* are insensitive to it indicating that the weak magnetic coupling observed is of intramolecular nature.

Dealing with the second point, when more than one unpaired electron per metal atom occurs, the experimental *J* parameter has to be decomposed into a sum of individual contributions, $J_{\mu\nu}$, involving each pair of magnetic orbitals implicated in the exchange phenomenon [equation (1)][44] where *n* is the number

$$J = 1/n^2 \sum_{\mu,\nu}^{n} J_{\mu\nu} \qquad (1)$$

of unpaired electrons of the metal centre. According to this equation, the net antiferromagnetic interaction is properly defined by $n^2J$, which is also included in Table 3. In general, for several families of homodinuclear compounds with a common bridge and different metal ions, the values observed of $n^2|J|$ are not constant and usually decrease when going from copper(II) to manganese(II). This trend can easily be understood taking into account the increasing number of ferromagnetic terms $J_{\mu\nu}$ in equation (1) involving pairs of orthogonal magnetic orbitals for the added unpaired electron and the increase in the energy of the d orbitals when going from copper(II) to manganese(II). The combination of these two factors leads to a progressive decrease in spin-density delocalization on the bridge and so to a decrease in the corresponding $J_{\mu\nu}$ terms in equation (1). However, one can see in Table 3 that $n^2|J|$ slightly increases in the bipy complexes (**1**, **3** and **4**). In this family of isostructural compounds the ta adopts a bis-bidentate bridging mode as shown in Scheme 2. For complex **1**, one of the two Cu–O (carboxylate) bonds is very long and so the magnetic orbital is in the *xz* plane (that is orthogonal to the terephthalate plane), whereas in the other two complexes there is a magnetic orbital in the

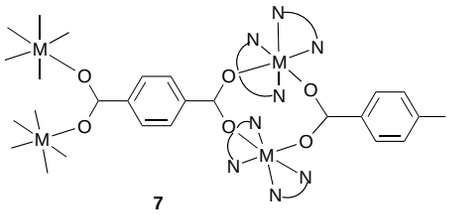

7

**Scheme 3**

*xy* plane (that is parallel to the terephthalate plane). Keeping in mind these features and taking into account that $J \propto S^2$ ($S$ being the overlap integral between the magnetic orbitals centred on each metal ion),[45,46] the overlapping through tetrephthalate in complexes **3** and **4** is twice that in **1**. Consequently, it is clear that $n^2|J|$ for **3** and **4** should be greater than that for **1**, as is observed. The fact $n^2|J|$ for **3** and **4** is not four times that of **1** (because of $J \propto S^2$) is due to the above-mentioned reasons. In complex **5** only one carboxylate oxygen is co-ordinated to the manganese(II) and the $n^2|J|$ value is smaller than that for **1**, as expected.

The last point is the increase in the antiferromagnetic coupling in complex **6** with respect to that in **5**. The value of the exchange coupling in **6** is very close to that observed in **7**[30] where each carboxylate group is linked to two manganese atoms in a *syn-syn* conformation leading to a chain of ta-bridged manganese(II) pairs as shown in Scheme 3. Most likely, the loss of the co-ordinated water molecule in **5** to yield **6** causes such a dimerization through each carboxylate and accounts for the observed coupling. Unfortunately, we have not got single crystals of complex **6** but the IR and magnetic data together with the structural knowledge of **7** strongly support the dimerization through carboxylate on each side of the benzene ring of the terephthalate and we suggest that **6** and **7** could present a similar structure. It is interesting that the common procedure to perform variable-temperature magnetic measurements (that is making a vacuum around the holder and purging with helium) cannot be used in the case of complex **5** because of the easy loss of the two co-ordinated water molecules which is assisted by carboxylate co-ordination. So, the magnetic properties of **5** were measured without applying any vacuum on the holder. If a vacuum is applied transformation into **6** takes place. The complete transformation is dependent on the time the vacuum is operating. The extent of transformation of **5** into **6** can easily be detected because of the amount of impurities revealed by the susceptibility curve of **6**. The data given in Table 3 concerning complex **6** were obtained after half a day under vacuum and only *ca.* 0.8% of impurity (as complex **5**) is present.

Concerning the two complexes of formula $[Cu_2(bipy)_2(H_2O)_2(ta)][ClO_4]_2$ and $[Cu_2(tmtacn)_2(H_2O)_2(ta)][ClO_4]_2$ from Table 4, only the structure of the last one is known[19,24] and corresponds to Scheme 4(*a*) where one of the two carboxylate oxygens is bound to copper(II) and the other is hydrogen bonded to a co-ordinated water molecule. The type of terephthalato co-ordination shown in Scheme 4(*a*) has been proposed as the driver of the relatively strong antiferromagnetic coupling observed in $[Cu_2(tmtacn)_2(H_2O)_2(ta)][ClO_4]_2$[24] and on this basis the same structural pattern was proposed for the penultimate compound of Table 4. It is very interesting that **5** exhibits the same type of terephthalate co-ordination. Consequently, if the presence of the intramolecular O–H···O bond in $[Cu_2(tmtacn)_2(H_2O)_2(ta)][ClO_4]_2$ causes the strong antiferromagnetic coupling observed for this compound as suggested,[24] one can easily predict a value of $J = -5.6$ cm$^{-1}$ for **5** (that is −140/25, see Table 3). Our results show that this is not the case ($J$ for **5** is −0.065). Moreover, we have performed extended-Hückel calculations on the model compounds shown

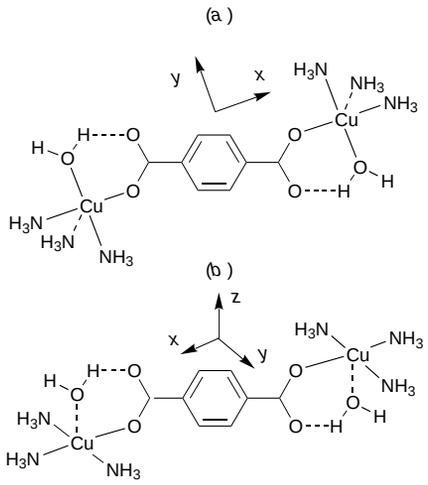

**Scheme 4**

in Schemes 2 and 4 and a very small and nearly identical energy gap between the singly occupied molecular orbitals (SOMOs) was found for the models in Scheme 4(*a*) and 4(*b*) revealing that the magnetic coupling should be very weak and similar in these cases. A somewhat greater energy gap was found for the model in Scheme 2. Self-consistent field Møller–Plesset (SCF-MP) calculations performed by Erasmus and Haase[47] are in agreement with our results. They calculated that the $J$ value for the last compound of Table 4 is in the range −0.085 to +0.057 cm$^{-1}$. In summary, our feeling is that the relatively strong antiferromagnetic coupling observed for the last two compounds in Table 4 is that they exhibit the same phenomenon that we have observed for **5** and **6**: carboxylate-assisted loss of the co-ordinated water molecule and subsequent carboxylate dimerization in the vacuum. In fact, the high percentage of impurities which were detected in the magnetic study of $[Cu_2(tmtacn)_2(H_2O)_2(ta)][ClO_4]_2$ could be due to a non-total dehydration.

Finally, we tried to prepare single crystals of the last compound of Table 4 by following the reported procedure and so check that it exhibits a relatively strong antiferromagnetic coupling only after loss of its co-ordinated water molecule under vacuum, leading to the *syn-syn* carboxylate bridging. Unfortunately, all our attempts led to a mixture of different ta-containing complexes of polymeric nature.

## Conclusion

Taking into account that the most favourable bridging mode of terephthalate to mediate exchange coupling is the bis-bidentate mode shown in Scheme 2 as indicated by Hückel calculations and given that it is unable to transmit a relatively large coupling, as shown experimentally (this is the heart of our contribution), we conclude that the terephthalate bridge is not a suitable bridging unit to mediate significant exchange coupling in contrast to what was suggested previously. The relatively large magnetic coupling observed in some of its copper(II) complexes is most likely due to a carboxylate-assisted loss of co-ordinated water molecules with subsequent carboxylate bridging in a *syn-syn* conformation.

## Acknowledgements

Financial support from the Spanish Dirección General de Investigación Científica y Técnica (Project PB-94-1002), the Italian Ministero dell'Università e della Ricerca Scientifica e Tecnologica and the Human Capital and Mobility Program (Network on Magnetic Molecular Materials from EEC) through grant ERBCHRX-CT920080 is gratefully acknowledged. One of us (J. C.) thanks the Ministerio Español de Educación y Ciencia for a predoctoral fellowship.

## References


1 *Magneto-Structural Correlations in Exchange Coupled Systems*, eds. R. D. Willet, D. Gatteschi and O. Kahn, Reidel, Dordrecht, 1985.
2 O. Kahn, *Molecular Magnetism*, VCH, Weinheim, 1993.
3 W. E. Hatfield, in *Magneto-Structural Correlations in Exchange Coupled Systems*, eds. R. D. Willet, D. Gatteschi and O. Kahn, Reidel, Dordrecht, 1985, p. 555.
4 V. M. Crawford, M. W. Richardson, J. R. Wasson, D. J. Hodgson and W. E. Hatfield, *Inorg. Chem.*, 1976, **15**, 2107.
5 R. E. Coffman and G. R. Buettner, *J. Phys. Chem.*, 1979, **18**, 2387.
6 N. F. Curtis, I. R. N. McCormick and T. N. Waters, *J. Chem. Soc., Dalton Trans.*, 1973, 1537.
7 T. R. Felthouse, E. J. Laskowski and D. N. Hendrickson, *Inorg. Chem.*, 1977, **16**, 1077.
8 M. Julve, M. Verdaguer, A. Gleizes, M. Philoche-Levisalles and O. Kahn, *Inorg. Chem.*, 1984, **23**, 3808.
9 M. Verdaguer, O. Kahn, M. Julve and A. Gleizes, *Nouv. J. Chim.*, 1985, **9**, 325.
10 H. Okawa, N. Matsumoto, M. Koikawa, K. Takeda and S. Kida, *J. Chem. Soc., Dalton Trans.*, 1990, 1383.
11 J. J. Girerd, S. Jeannin, Y. Jeannin and O. Kahn, *Inorg. Chem.*, 1978, **17**, 3034.
12 R. Vicente, J. Ribas, S. Alvarez, A. Seguí, X. Solans and M. Verdaguer, *Inorg. Chem.*, 1987, **26**, 4004.
13 X. Solans, M. Aguiló, A. Gleizes, J. Faus, M. Julve and M. Verdaguer, *Inorg. Chem.*, 1990, **29**, 775.
14 I. Castro, J. Sletten, J. Faus, Y. Journaux, F. Lloret and S. Alvarez, *Inorg. Chem.*, 1992, **31**, 1889.
15 F. Tinti, M. Verdaguer, O. Kahn and J. M. Savariault, *Inorg. Chem.*, 1987, **26**, 2380.
16 O. Kahn, *Angew. Chem.*, 1985, **97**, 837; *Angew. Chem., Int. Ed. Engl.*, 1985, **24**, 834 and refs. therein.
17 M. Julve, M. Verdaguer, J. Faus, F. Tinti, J. Moratal, A. Monge and E. Gutiérrez-Puebla, *Inorg. Chem.*, 1987, **26**, 3520.
18 T. R. Felthouse, T. Y. Dong, D. N. Hendrickson, H. S. Shieh and M. R. Thompson, *J. Am. Chem. Soc.*, 1986, **108**, 8201.
19 P. Chaudhuri, K. Oder, K. Wieghardt, S. Gehring, W. Haase, B. Nuber and J. Weiss, *J. Am. Chem. Soc.*, 1988, **110**, 3657.
20 M. Verdaguer, J. Gouteron, S. Jeannin, Y. Jeannin and O. Kahn, *Inorg. Chem.*, 1984, **23**, 4291.
21 E. G. Bakalbassis, C. Tsipis, A. Bozopoulos, W. Dreisig, H. Hartl and J. Mrozinski, *Inorg. Chim. Acta*, 1991, **186**, 113.
22 C. E. Xanthopoulos, M. P. Sigalas, G. A. Katsoulos, C. A. Tsipis, A. Terzis, M. Mentzafos and A. Hountas, *Inorg. Chem.*, 1993, **32**, 5433.
23 E. G. Bakalbassis and C. A. Tsipis, *Inorg. Chem.*, 1985, **24**, 4231.
24 K. S. Bürger, P. Chaudhuri, K. Wieghardt and B. Nuber, *Chem. Eur. J.*, 1995, **1**, 583.
25 Z. L. Deng, J. Shi, Z. H. Jiang, D. Z. Liao, S. P. Yan, G. L. Wang, H. G. Wang and R. J. Wang, *Polyhedron*, 1992, **11**, 885.
26 A. C. T. North, D. C. Philips and F. S. Mathews, *Acta Crystallogr., Sect. A*, 1968, **24**, 351.
27 SHELXTL PLUS, Version 4.11/V, Siemens Analytical X-ray Instruments Inc., Madison, WI, 1990.
28 M. Nardelli, *Comput. Chem.*, 1983, **7**, 95.
29 G. B. Deacon and R. J. Phillips, *Coord. Chem. Rev.*, 1980, **33**, 227.
30 J. Cano, G. De Munno, J. Sanz, R. Ruiz, F. Lloret, J. Faus and M. Julve, *J. Chem. Soc., Dalton Trans.*, 1994, 3465.
31 L. L. Merrit and D. Schroeder, *Acta Crystallogr.*, 1956, **9**, 801.
32 E. G. Bakalbassis, A. P. Bozopoulos, J. Mrozinski, P. J. Rentzaperis and C. A. Tsipis, *Inorg. Chem.*, 1988, **27**, 529.
33 D. P. Anderson, A. B. Packard and M. Nicolas, *Inorg. Chem.*, 1976, **15**, 1613.
34 I. Castro, J. Faus, M. Julve and A. Gleizes, *J. Chem. Soc., Dalton Trans.*, 1991, 1937 and refs. therein.
35 T. J. R. Weakley, *Acta Crystallogr., Sect. B*, 1978, **34**, 3756.
36 S. R. Holleman, O. J. Parker and G. L. Breneman, *Acta Crystallogr., Sect. C*, 1994, **50**, 867.
37 A. P. Ginsberg, R. L. Martin, R. W. Brookes and R. C. Sherwood, *Inorg. Chem.*, 1972, **11**, 2884.
38 G. De Munno, M. Julve, F. Lloret and A. Derory, *J. Chem. Soc., Dalton Trans.*, 1993, 1179.
39 M. E. Lines, *J. Chem. Phys.*, 1971, **55**, 2977.
40 E. Coronado, M. Drillon, P. R. Nugteren, L. J. de Jongh and D. Beltrán, *J. Am. Chem. Soc.*, 1988, **110**, 3907.
41 G. De Munno, M. Julve, F. Lloret, J. Faus and A. Caneschi, *J. Chem. Soc., Dalton Trans.*, 1994, 1175.
42 E. G. Bakalbassis, J. Mrozinski and C. A. Tsipis, *Inorg. Chem.*, 1986, **25**, 3684.
43 E. G. Bakalbassis, P. Bergerat, O. Kahn, S. Jeannin, Y. Jeannin, Y. Dromzee and M. Guillot, *Inorg. Chem.*, 1992, **31**, 625.
44 O. Kahn, *Struct. Bonding* (*Berlin*), 1987, **68**, 89 and refs. therein.
45 J. J. Girerd, M. F. Charlot and O. Kahn, *Mol. Phys.*, 1977, **34**, 1063.
46 O. Kahn and M. F. Charlot, *Nouv. J. Chim.*, 1980, **4**, 567.
47 C. Erasmus and W. Haase, *Spectrochim. Acta, Part A*, 1994, **50**, 2189.


*Received* 14*th January* 1997; *Paper* 7/00323D